Acta Crystallographica Section F
Structural Biology and Crystallization Communications
ISSN 1744-3091

Crystallization and preliminary X-ray analysis of the *Clostridium botulinum* type D nontoxic nonhaemagglutinin

Keita Miyata,[a] Ken Inui,[a] Shin-Ichiro Miyashita,[a] Yoshimasa Sagane,[a] Kimiko Hasegawa,[b] Takashi Matsumoto,[b] Akihito Yamano,[b] Koichi Niwa,[a] Toshihiro Watanabe[a]* and Tohru Ohyama[a]*

[a]Department of Food and Cosmetic Science, Faculty of Bioindustry, Tokyo University of Agriculture, 196 Yasaka, Abashiri, Hokkaido 099-2493, Japan, and [b]Rigaku Corporation, 3-9-12 Matsubara-Cho, Akishima, Tokyo 196-8666, Japan

Correspondence e-mail: t-watana@bioindustry.nodai.ac.jp, t-oyama@bioindustry.nodai.ac.jp

Received 28 November 2011
Accepted 28 December 2011

Clostridium botulinum produces botulinum neurotoxin (BoNT) as a large toxin complex assembled with nontoxic nonhaemagglutinin (NTNHA) and/or haemagglutinin components. Complex formation with NTNHA is considered to be critical in eliciting food poisoning because the complex shields the BoNT from the harsh conditions in the digestive tract. In the present study, NTNHA was expressed in *Escherichia coli* and crystallized. Diffraction data were collected to 3.9 Å resolution. The crystal belonged to the trigonal space group $P321$ or $P3_121/P3_221$, with unit-cell parameters $a = b = 147.85$, $c = 229.74$ Å. The structure of NTNHA will provide insight into the assembly mechanism that produces the unique BoNT–NTNHA complex.

1. Introduction

Botulinum neurotoxin (BoNT; 150 kDa) is a potent toxin produced by the anaerobic Gram-positive bacterium *Clostridium botulinum* as seven related but serologically distinct proteins designated serotypes A–G. After the ingestion of BoNT-contaminated food, BoNT passes through the gastrointestinal tract and ultimately reaches the neuromuscular junctions, where it binds to the presynaptic membrane and is internalized into nerve cells by receptor-mediated endocytosis. The Zn^{2+}-endopeptidase activity of BoNT cleaves specific sites on target proteins (*e.g.* synaptobrevin/VAMP, syntaxin and SNAP-25), blocking the docking and fusion of synaptic vesicles and leading to inhibition of neurotransmitter release (Montecucco & Schiavo, 1993). This process causes muscular paralysis in humans and animals, leading to the disease botulism.

In culture supernatants or naturally contaminated foods, BoNT ordinarily forms a noncovalent toxin complex (TC) with nontoxic proteins, including a single nontoxic nonhaemagglutinin (NTNHA; 130 kDa) and/or three types of haemagglutinin (HA) subcomponents: HA-70, HA-33 and HA-17 (70, 33 and 17 kDa, respectively). Depending on the serotype, the TC can be found in three forms: the 750 kDa L-TC (a complex of BoNT, NTNHA, HA-70, HA-33 and HA-17), LL-TC (probably a dimer of L-TC) and the 280 kDa M-TC (a complex of BoNT and NTNHA) (Oguma *et al.*, 1999). It has been reported that TC species for all serotypes dissociated into two molecules, a BoNT and a set of nontoxic components (NTNHA for M-TC or NTNHA/HAs for L-TC), under alkaline conditions above pH 7.2.

Previous experiments have demonstrated that the TC protects BoNT during exposure to harsh conditions (Niwa *et al.*, 2007). Most proteins are degraded into short peptides and amino acids in the stomach and small intestine during the process of digestion. TC is also exposed to acidic (pH 2) gastric juices containing the protease pepsin in the stomach and then enters the small intestine, where it encounters several more proteases. However, despite these denaturing and proteolytic conditions, BoNT and the other nontoxic components can subsequently be detected in the blood and circulatory systems (Kitamura *et al.*, 1969; Sakaguchi *et al.*, 1984), with NTNHA and HAs

seeming to function as delivery vehicles for BoNT trafficking. The formation of this complex is considered to be critical in eliciting food poisoning because it shields the BoNT molecule from acidic conditions and proteases in the stomach (Sakaguchi *et al.*, 1984; Miyata *et al.*, 2009), while the HA subcomponents play an essential role in the effective absorption of TCs by the small intestine (Fujinaga *et al.*, 1997). Thus, NTNHA plays a role in shielding BoNT from proteases and connects the BoNT and HA subcomponents to form L-TC.

The NTNHAs of M-TC produced by serotype A (Fujita *et al.*, 1995), C (Sagane *et al.*, 2000) and D (Ohyama *et al.*, 1995; Sagane *et al.*, 2000) strains have always been found to be nicked at a unique site, while those of L-TC exist as an unprocessed single-chain polypeptide. Recently, we found that a unique strain, serotype D strain 4947 (D-4947), produces intact M-TC and L-TC without nicking in the subcomponents (Sagane *et al.*, 2002). In addition, we inadvertently found that when isolated NTNHA or NTNHA in M-TC were incubated for long periods at 298 K, the NTNHA was spontaneously converted to the nicked form, with NTNHA detectable as 15 and 115 kDa bands on SDS–PAGE (Sagane *et al.*, 2002).

To date, the crystal structures of several BoNT serotypes (Lacy *et al.*, 1998; Swaminathan & Eswaramoorthy, 2000), including the serotype C HA-70 protein (Nakamura *et al.*, 2009) and the serotype D HA-33–HA-17 complex (Hasegawa *et al.*, 2007), have been determined. However, the structure of NTNHA has not yet been determined for the five botulinum TC components, which encourages us to examine using X-ray crystallography the mechanism by which BoNT is protected from proteases. We believe that analysis of the NTNHA structure will elucidate the mechanism by which BoNT, NTNHA and HAs assemble to form the TC, as well as the molecular mechanism of spontaneous NTNHA processing. Here, we describe the crystallization and preliminary X-ray diffraction studies of D-4947 NTNHA.

2. Materials and methods

2.1. Production and purification of D-4947 NTNHA

For crystallization, NTNHA was expressed as a His-tag fusion protein (recombinant NTNHA; rNTNHA) which contains 35 tag residues including a 6×His tag (pET200/D-TOPO; Invitrogen) and was purified using affinity and gel-filtration column chromatography as described previously (Miyata *et al.*, 2009). The cells were grown in 1 l Luria–Bertani (LB) medium to an OD_{600} of 0.5 and NTNHA expression was then induced by the addition of isopropyl β-D-1-thiogalactopyranoside (IPTG) to a final concentration of 0.1 m*M*. Induction was allowed to proceed at 291 K for 18 h. The cells were suspended in 80 ml 50 m*M* sodium phosphate buffer pH 7.4 containing 0.3 *M* NaCl. The cell suspension was then sonicated and centrifuged at 10 000*g* for 20 min at 277 K. The following purification steps were all carried out at room temperature. The rNTNHA was purified from the resulting supernatant using an Ni-Charged Resin (Bio-Rad) affinity column. The rNTNHA was then further purified using a HiLoad 16/60 Superdex 200 pg (GE Healthcare) gel-filtration column equilibrated with 50 m*M* sodium phosphate buffer pH 6.0 containing 0.15 *M* NaCl to remove contaminating proteins. Successive 1 l cultures typically yielded about 1 mg rNTNHA (Miyata *et al.*, 2009).

The rNTNHA is spontaneously nicked at a unique site, leading to the appearance of two bands at 18 and 115 kDa on SDS–PAGE, as previously reported (Miyata *et al.*, 2009). Therefore, rNTNHA was prepared as a spontaneously nicked form. The purified rNTNHA was incubated at 298 K for 12 d and then purified to remove contaminants on a HiLoad 16/60 Superdex 200 pg gel-filtration column equilibrated with 50 m*M* sodium phosphate buffer pH 6.0 containing 0.15 *M* NaCl and on a Mono S HR 5/5 column (GE Healthcare) equilibrated with 50 m*M* sodium acetate buffer pH 5.0 followed by elution with an NaCl gradient from 0 to 0.4 *M*. The nicked form of rNTNHA was assessed by SDS–PAGE.

2.2. Crystallization and X-ray data collection

Crystals were grown by the hanging-drop vapour-diffusion method (Adachi *et al.*, 2003) at 293 K. For crystallization of rNTNHA, the protein solution was concentrated to a minimal volume using Amicon Ultra-0.5 with a molecular-weight cutoff of 10 kDa and diluted to 5.5 mg ml^{-1} in 50 m*M* acetate buffer pH 5.0 without any additional salt. The rNTNHA solution was filtered through an Ultrafree-MC 0.22 µm filter unit (Millipore). Initial crystallization screening of rNTNHA was performed using Crystal Screen (Hampton Research). Each reservoir solution (500 µl) was transferred into a VDX plate (Hampton Research) and the wells were individually sealed with cover glasses with crystallization drops. The crystallization drop consisted of 3.0 µl protein solution and 2.0 µl crystallization reservoir solution consisting of 0.2 *M* ammonium sulfate, 30%(*w*/*v*) polyethylene glycol monomethyl ether 2000 in 0.1 *M* sodium acetate trihydrate buffer pH 4.6. Crystals were immediately flash-cooled in a stream of gaseous nitrogen at 100 K without addition of cryoprotectant. Diffraction data were collected using a Rigaku R-AXIS VII image-plate detector and an FR-E$^+$ SuperBright X-ray generator. Data reduction was performed using the *CrystalClear* v.2.0 software package (Rigaku).

2.3. Self-rotation function calculation

A self-rotation function was calculated using *MOLREP* (Vagin & Teplyakov, 2010) in the resolution range 31–4 Å; the integration radius was set to 60 Å.

3. Results and discussion

The BoNT, NTNHA and HA-70 subcomponents of the BoNT complex species produced by serotype A, C and D strains have always been found to be nicked at specific sites by endogenous bacterial proteases (Oguma *et al.*, 1999). Recently, we found that unlike other strains, D-4947 uniquely produces a considerable amount of BoNT

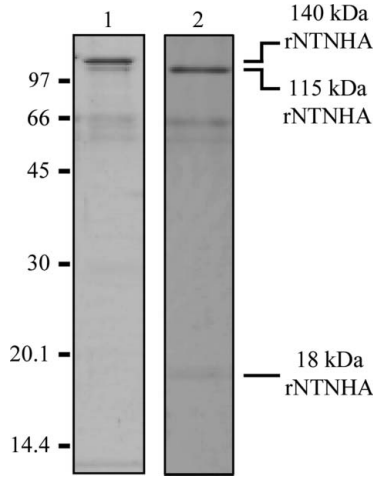

Figure 1
SDS–PAGE of purified rNTNHA and spontaneously nicked rNTNHA. Lane 1, purified rNTNHA. Lane 2, spontaneously nicked rNTNHA. The positions of molecular-weight markers are labelled on the left in kDa.

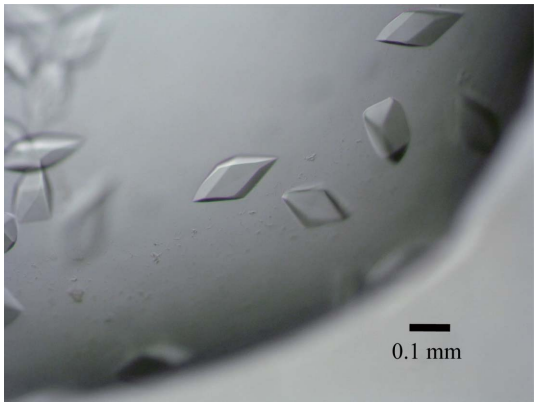

Figure 2
Crystals of rNTNHA as grown by the hanging-drop vapour-diffusion method. The average dimensions of these crystals were 0.2 × 0.2 × 0.1 mm.

complex that has no nicking in any component (Kouguchi *et al.*, 2002; Hasegawa *et al.*, 2004). However, in both the isolated form and in the BoNT–NTNHA complex D-4947 NTNHA was found to be gradually converted to the nicked NTNHA form owing to spontaneous cleavage during long-term storage in the refrigerator, leading to 15 and 115 kDa fragments on SDS–PAGE and to the excision of several amino acids at specific sites (Sagane *et al.*, 2000, 2002). We recently constructed an *E. coli* expression system for D-4947 NTNHA, in which it also appeared as the spontaneously nicked form (Miyata *et al.*, 2009). Thus, incubation of rNTNHA for crystallization induces conversion from the intact to the nicked form. To avoid generating a mixture of intact and nicked forms, rNTNHA was incubated for long periods at 298 K without addition of protease. SDS–PAGE analysis showed that the disappearance of the 140 kDa band was accompanied by the appearance of 18 and 115 kDa bands (Fig. 1). The nicked-form rNTNHA is a binary complex with 115 and 18 kDa fragments bound tightly to each other (Miyata *et al.*, 2009). In this study, the spontaneously nicked form of rNTNHA was used for crystallization.

Table 1
Data-collection statistics.

Values in parentheses are for the highest resolution shell.

Wavelength (Å)	1.5418
Temperature (K)	100
Resolution (Å)	31.08–3.90 (4.04–3.90)
No. of observed reflections	79904
No. of unique reflections	25867
Completeness (%)	95.7 (95.7)
$R_{\rm merge}$ †	17.4 (35.6)
$\langle I/\sigma(I)\rangle$	4.5 (2.3)
Space group	$P321$ or $P3_121/P3_221$
Unit-cell parameters (Å)	$a = b = 147.85$, $c = 229.74$

† $R_{\rm merge} = \sum_{hkl}\sum_i |I_i(hkl) - \langle I(hkl)\rangle| / \sum_{hkl}\sum_i I_i(hkl)$, where $\langle I(hkl)\rangle$ is the mean intensity of multiple observations of symmetry-related reflections.

Crystals appeared within 3 d of incubation and grew to maximum dimensions of 0.2 × 0.2 × 0.1 mm (Fig. 2). Diffraction data were obtained under cryoconditions and a full set of intensity data was collected at 3.9 Å resolution (Fig. 3*a*). Data-collection statistics and crystal data are summarized in Table 1. The data showed that the crystal belonged to the trigonal space group $P321$ or $P3_121/P3_221$. A self-rotation function map (Fig. 3*b*) displayed peaks in the $\chi = 180^\circ$ section, indicating noncrystallographic symmetric axes between two molecules in the asymmetric unit. Assuming that the space group is $P321$, the most plausible results suggest that there are two molecules in the asymmetric unit. The Matthews coefficient is 2.79 Å^3 Da^{-1} (Matthews, 1968), with a solvent content of 55.91% as determined using *MATTHEWS_COFF* from the *CCP*4 software package (Winn *et al.*, 2011). We are currently preparing heavy-atom derivatives for multiple anomalous scattering phasing. The association of BoNT and NTNHA forms M-TC in a pH-dependent manner, which results in a

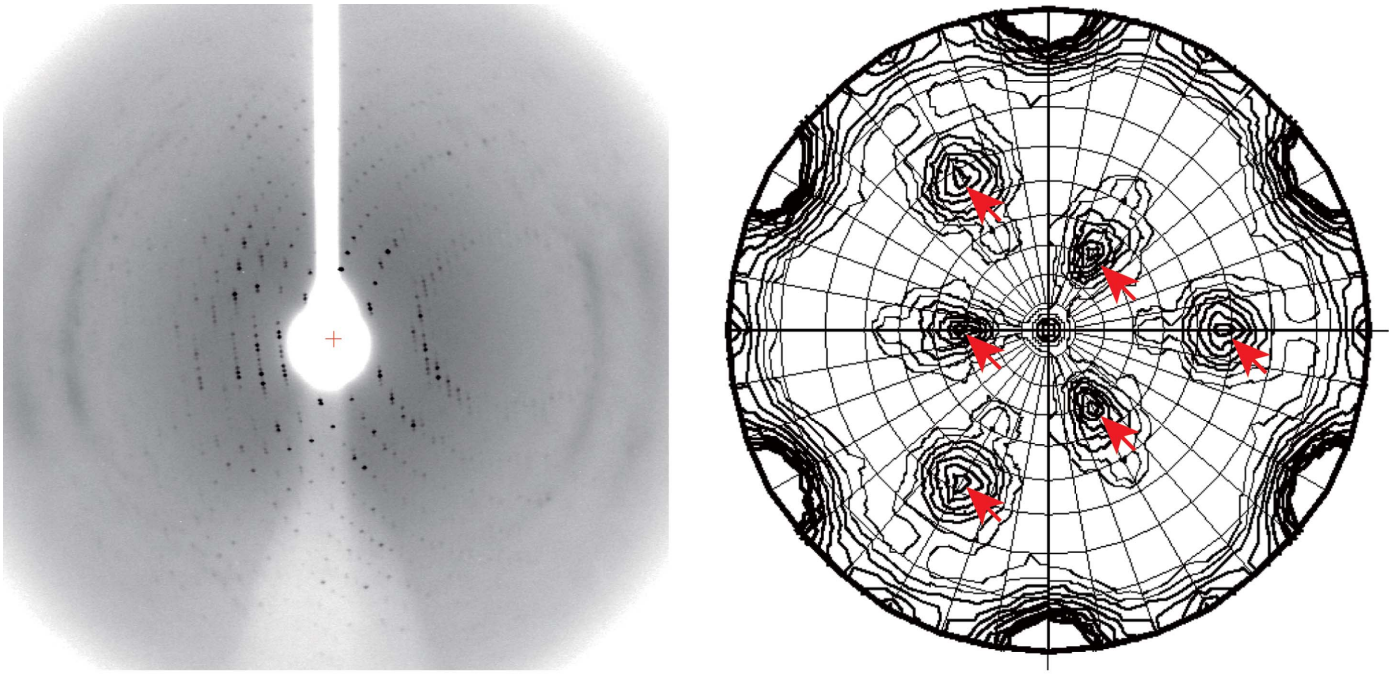

(*a*) (*b*)

Figure 3
(*a*) An X-ray diffraction image from an rNTNHA crystal. The edge of the detector corresponds to a resolution of 3.9 Å. An oscillation angle of 0.5° was used. (*b*) A self-rotation function map of rNTNHA diffraction data plotted at $\chi = 180^\circ$. The related noncrystallographic twofold axes are indicated by arrows.

proteolytically stable complex. It would be worthwhile crystallizing M-TC, which is under way in our laboratory, in order to understand the assembly mechanism that produces the unique BoNT–NTNHA complex and the stability of the complex.

The authors would like to thank Mr Ryohta Horiuchi, Mr Masashi Muramatsu, Mr Takumi Yamazaki and Mr Keisuke Nakauchi for their technical assistance. This work was supported by a Research Fellowship from the Japan Society for Promotion of Science (JSPS) for Young Scientists (46108836C).

References

Adachi, H., Takano, K., Morikawa, M., Kanaya, S., Yoshimura, M., Mori, Y. & Sasaki, T. (2003). *Acta Cryst.* D**59**, 194–196.
Fujinaga, Y., Inoue, K., Watanabe, S., Yokota, K., Hirai, Y., Nagamachi, E. & Oguma, K. (1997). *Microbiology*, **143**, 3841–3847.
Fujita, R., Fujinaga, Y., Inoue, K., Nakajima, H., Kumon, H. & Oguma, K. (1995). *FEBS Lett.* **376**, 41–44.
Hasegawa, K., Watanabe, T., Sato, H., Sagane, Y., Mutoh, S., Suzuki, T., Yamano, A., Kouguchi, H., Takeshi, K., Kamaguchi, A., Fujinaga, Y., Oguma, K. & Ohyama, T. (2004). *Protein J.* **23**, 371–378.
Hasegawa, K., Watanabe, T., Suzuki, T., Yamano, A., Oikawa, T., Sato, Y., Kouguchi, H., Yoneyama, T., Niwa, K., Ikeda, T. & Ohyama, T. (2007). *J. Biol. Chem.* **282**, 24777–24783.
Kitamura, M., Sakaguchi, S. & Sakaguchi, G. (1969). *J. Bacteriol.* **98**, 1173–1178.
Kouguchi, H., Watanabe, T., Sagane, Y., Sunagawa, H. & Ohyama, T. (2002). *J. Biol. Chem.* **277**, 2650–2656.
Lacy, D. B., Tepp, W., Cohen, A. C., DasGupta, B. R. & Stevens, R. C. (1998). *Nature Struct. Biol.* **5**, 898–902.
Matthews, B. W. (1968). *J. Mol. Biol.* **33**, 491–497.
Miyata, K., Yoneyama, T., Suzuki, T., Kouguchi, H., Inui, K., Niwa, K., Watanabe, T. & Ohyama, T. (2009). *Biochem. Biophys. Res. Commun.* **384**, 126–130.
Montecucco, C. & Schiavo, G. (1993). *Trends Biochem. Sci.* **18**, 324–327.
Nakamura, T., Kotani, M., Tonozuka, T., Ide, A., Oguma, K. & Nishikawa, A. (2009). *J. Mol. Biol.* **385**, 1193–1206.
Niwa, K., Koyama, K., Inoue, S., Suzuki, T., Hasegawa, K., Watanabe, T., Ikeda, T. & Ohyama, T. (2007). *FEMS Immunol. Med. Microbiol.* **49**, 346–352.
Oguma, K., Inoue, K., Fujinaga, Y., Yokota, K., Watanabe, T., Ohyama, T., Takeshi, K. & Inoue, K. (1999). *J. Toxicol. Toxin Rev*, **18**, 17–34.
Ohyama, T., Watanabe, T., Fujinaga, Y., Inoue, K., Sunagawa, H., Fujii, N., Inoue, K. & Oguma, K. (1995). *Microbiol. Immunol.* **39**, 457–465.
Sagane, Y., Watanabe, T., Kouguchi, H., Sunagawa, H., Inoue, K., Fujinaga, Y., Oguma, K. & Ohyama, T. (2000). *J. Protein Chem.* **19**, 575–581.
Sagane, Y., Watanabe, T., Kouguchi, H., Sunagawa, H., Obata, S., Oguma, K. & Ohyama, T. (2002). *Biochem. Biophys. Res. Commun.* **292**, 434–440.
Sakaguchi, G., Kozaki, S. & Ohishi, I. (1984). *Bacterial Protein Toxins*, edited by J. E. Alouf, F. J. Fehrenbach, J. H. Freer & J. Jeljiaszwicz, pp. 435–443. London: Academic Press.
Swaminathan, S. & Eswaramoorthy, S. (2000). *Nature Struct. Biol.* **7**, 693–699.
Vagin, A. & Teplyakov, A. (2010). *Acta Cryst.* D**66**, 22–25.
Winn, M. D. *et al.* (2011). *Acta Cryst.* D**67**, 235–242.